0026-895X/07/7202-327–340$20.00
MOLECULAR PHARMACOLOGY
Vol. 72, No. 2
35543/3235493
Mol Pharmacol 72:327–340, 2007
Printed in U.S.A.

Molecular Interaction of a Potent Nonpeptide Agonist with the Chemokine Receptor CCR8

Pia C. Jensen, Rie Nygaard, Stefanie Thiele, Amy Elder, Guoming Zhu, Roland Kolbeck, Shomir Ghosh, Thue W. Schwartz, and Mette M. Rosenkilde

Laboratory for Molecular Pharmacology, Department of Pharmacology, Copenhagen University, Copenhagen, Denmark (P.C.J., R.N., S.T., T.W.S., M.M.R.); and Millennium Pharmaceuticals, Massachusetts Institute of Technology, Cambridge, Boston, Massachusetts (A.E., G.Z., R.K., S.G.)

Received February 26, 2007; accepted May 16, 2007.

ABSTRACT

Most nonpeptide antagonists for CC-chemokine receptors share a common pharmacophore with a centrally located, positively charged amine that interacts with the highly conserved glutamic acid (Glu) located in position 6 of transmembrane helix VII (VII:06). We present a novel CCR8 nonpeptide agonist, 8-[3-(2-methoxyphenoxy)benzyl]-1-phenethyl-1,3,8-triaza-spiro[4.5]decan-4-one (LMD-009), that also contains a centrally located, positively charged amine. LMD-009 selectively stimulated CCR8 among the 20 identified human chemokine receptors. It mediated chemotaxis, inositol phosphate accumulation, and calcium release with high potencies (EC_{50} from 11 to 87 nM) and with efficacies similar to that of the endogenous agonist CCL1, and it competed for ^{125}I-CCL1 binding with an affinity of 66 nM. A series of 29 mutations targeting 25 amino acids broadly distributed in the minor and major ligand-binding pockets of CCR8 uncovered that the binding of LMD-009 and of four analogs [2-(1-(3-(2-methoxyphenoxy)benzyl)-4-hydroxypiperidin-4-yl)benzoic acid (LMD-584), *N*-ethyl-2-4-methoxybenzenesulfonamide (LMD-902), *N*-(1-(3-(2-methoxyphenoxy)benzyl)piperidin-4-yl)-2-phenyl-4-(pyrrolidin-1-yl)butanamide (LMD-268), and *N*-(1-(3-(2-methoxyphenoxy)benzyl)piperidin-4-yl)-1,2,3,4-tetrahydro-2-oxoquinoline-4-carboxamide (LMD-174)] included several key-residues for nonpeptide antagonists targeting CCR1, -2, and -5. It is noteworthy that a decrease in potency of nearly 1000-fold was observed for all five compounds for the Ala substitution of the anchor-point GluVII:06 (Glu^{286}) and a gain-of-function of 19-fold was observed for LMD-009 (but not the four other analogs) for the Ala substitution of PheVI:16 (Phe^{254}). These structural hallmarks were particularly important in the generation of a model of the molecular mechanism of action for LMD-009. In conclusion, we present the first molecular mapping of the interaction of a nonpeptide agonist with a chemokine receptor and show that the binding pocket of LMD-009 and of analogs overlaps considerably with the binding pockets of CC-chemokine receptor nonpeptide antagonists in general.

Chemokine receptors belong to the superfamily of rhodopsin-like G protein-coupled 7TM receptors (Murphy et al., 2000). The chemokine ligands (*chemo*tactic cyto*kines*) are a family of large peptides (70–80 amino acids in length) composed of around 50 members. The CC-chemokines are characterized by the absence of an amino acid between the first two of four conserved cysteines and constitute the largest group (CCL1–28), whereas the CXC-chemokines constitute the other major group (CXCL1–16). Two additional chemokines, the XCL1 and the CX3CL1, have been described previously (Murphy et al., 2000). The chemokine system regulates the development, activation, and recruitment of leukocytes and plays important roles outside the immune system (for instance, on organogenesis, angiogenesis, and carcinogenesis) (Gerard and Rollins, 2001). CCR8 is selectively expressed on a subset of T-helper-2 (Th2) and regulatory T cells and is upregulated on Th2 cells upon activation (Soler et al., 2006). Activated Th2 cells produce the cytokines IL-4, IL-5, and IL-13,

The study was supported by the Danish Research Council, the NovoNordisk Foundation, and the Aase og Einer Danielsen Foundation. The study was also supported by the European Community's Sixth Framework Program (grant LSHB-CT-2005-518167).

Article, publication date, and citation information can be found at http://molpharm.aspetjournals.org.

doi:10.1124/mol.107.035543.

ABBREVIATIONS: Th2, T-helper-2; IL, interleukin; CCL, CC-chemokine; CXCL, CXC-chemokine; ZK 756326, 2-[2-[4-(3-Phenoxybenzyl)piperazin-1-yl]ethoxy]ethanol; LMD-009, 8-[3-(2-methoxyphenoxy)benzyl]-1-phenethyl-1,3,8-triaza-spiro[4.5]decan-4-one; LMD-584, 2-(1-(3-(2-methoxyphenoxy)benzyl)-4-hydroxypiperidin-4-yl)benzoic acid; LMD-902, *N*-ethyl-2-4-methoxybenzenesulfonamide; LMD-268, *N*-(1-(3-(2-methoxyphenoxy)benzyl)piperidin-4-yl)-2-phenyl-4-(pyrrolidin-1-yl)butanamide; LMD-174, *N*-(1-(3-(2-methoxyphenoxy)benzyl)piperidin-4-yl)-1,2,3,4-tetrahydro-2-oxoquinoline-4-carboxamide; 7TM receptors, 7 transmembrane spanning α-helix receptors; TM, transmembrane; Gqi4myr, G$\alpha\Delta$6qi4myr; IP, inositol phosphates; TBS, Tris-buffered saline; BX471, (*R*)-*N*-[5-chloro-2-[2-[4-[(4-fluorophenyl)methyl]-2-methyl-1-piperazinyl]-2-oxoethoxy]phenyl]-urea; wt, wild type; ELISA, enzyme-linked immunosorbent assay.

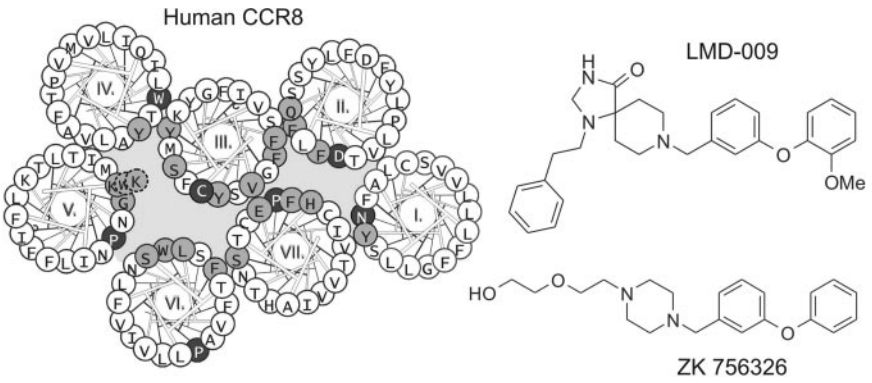

Fig. 1. Helical wheel diagram of CCR8 together with the structures of the two identified CCR8 receptor nonpeptide agonists, LMD-009 and ZK 756326. The circles with grey background in the helical wheel diagram indicate mutations performed in the present study. The circles with black background indicate conserved residues within the rhodopsin-like 7TM receptors. The structure of LMD-009 is shown together with the structure of the recently published CCR8 agonist ZK 756326 (Haskell et al., 2006).

which are important mediators of inflammation and airway hyper-reactivity in bronchial asthma, and CCR8 deficiency has been shown to ameliorate lung inflammation and airway function in the mouse (Chensue et al., 2001). CCR8 also seems to play an important role in pathologic conditions of the central nervous system in that it is expressed on phagocytic macrophages and activated microglial cells in the central nervous system, in active demyelinating multiple sclerosis, progressive multifocal leukoencephalopathy, and in cerebral ischemic lesions (Trebst et al., 2003).

In contrast to many other CC and CXC-chemokine receptors, which are rather promiscuous in their ligand-binding profile, CCR8 binds only one endogenous chemokine, CCL1 (I-309), and CCL1 interacts only with this one receptor. There are only a few additional chemokine/receptor pairs with a similar stringency, for example CXCL12 (SDF-1)/CXCR4 and CX3CL1 (fractalkine)/CX3CR1 (Murphy et al., 2000). However, additional virus-encoded CC-chemokines targeting CCR8 have been described, indicating a potential role for CCR8 in infectious diseases. For example, the CCR8 antagonist MC148, encoded by the poxvirus *Molluscum contagiosum* (Damon et al., 1998; Luttichau et al., 2000) and the two CCR8 agonists, vCCL1 and vCCL2, encoded by human herpesvirus 8 (Dairaghi et al., 1999).

Many pharmaceutical companies wish to develop chemokine receptor nonpeptide antagonists because of the well documented functions of the chemokine system in immune system surveillance and pathological inflammatory processes. The research in chemokine nonpeptide antagonists has thus far resulted in ~250 patent applications and nine clinical trials (Horuk, 2003). Indeed, nonpeptide antagonists have today been identified for the majority of chemokine receptors. However, CCR8 differs from these in that agonists, instead of antagonists, appear from screening efforts (i.e., CCR8 is agonist-prone). Thus, a micromolar nonpeptide agonist, ZK 756326, has recently been described for CCR8 (Haskell et al., 2006), and vCCL2 (which in general acts like a broad-spectrum chemokine antagonist) also activates this receptor (Dairaghi et al., 1999). We present here a novel high-affinity nonpeptide agonist for CCR8, LMD-009, that acts in the nanomolar range with the same efficacy and potency as CCL1. The structure of LMD-009 has some similarities to that of ZK 756326 (Haskell et al., 2006). Both compounds contain a central amine—as observed for many chemokine receptor nonpeptide antagonists (Rosenkilde and Schwartz, 2006)—and an aromatic group (biphenyl) on the "right side"; the only difference is an *ortho*-methoxy group in the terminal phenyl of LMD-009. The central amine source differs slightly, because LMD-009 contains a spiro-ring system with a piperidine, whereas ZK 756326 contains a piperazine. The greatest difference is found on the "left side, " in that LMD-009 contains an aromatic group (phenethylimidazoline-4-one) that in ZK 756326 is an ethoxyethanol (Fig. 1). Mutational mapping of LMD-009 and a series of analogs of this in a library of 27 mutants covering the main ligand-binding pocket of CCR8 demonstrated that the highly conserved Glu at position 6 in the extracellular end of TM-VII (VII:06[1]) (Rosenkilde and Schwartz, 2006) is essential for the action of LMD-009. In addition, we find that aromatic residues in the binding pocket, which are believed to interact with the nonpeptide antagonists in other chemokine receptors, are also important for the binding of LMD-009.

Materials and Methods

Materials. CCR1 and -2, CXCR1, -2, and -4, and CX3CR1 were kindly provided by Timothy N. C. Wells (Serono Pharmaceuticals, Geneva, Switzerland). CCR3, -4, -6, -9, -10, and -11 were purchased from Origene (Rockville, MD). CXCR5 and CCR7 were kindly provided by Martin Lipp (Max Delbrück Center for Molecular Medicine, Berlin-Buch, Germany). CXCR3 was kindly provided by Kuldeep Neote (Pfizer, Groton, CT). XCR1 and CCR8 were kindly provided by Hans R. Lüttichau (Copenhagen University, Copenhagen, Denmark). The human chemokines were purchased from PeproTech (Rocky Hill, NJ) or from R&D Systems (Minneapolis, MN). The promiscuous chimeric G-protein $G\alpha\Delta_{6qi4myr}$ (abbreviated Gqi4myr) was kindly provided by Evi Kostenis (7TM Pharma A/S, Hørsholm, Denmark). [*myo*-^{3}H]inositol and ^{125}I-CCL1 were from GE Healthcare (Chalfont St. Giles, Buckinghamshire, UK). LMD-009 was provided by Millennium Pharmaceuticals.

Site-Directed Mutagenesis. The human CCR8 was inserted into the pcDNA3 eukaryotic expression vector or into the FLAG-pcDNA3.1 vector kindly provided by Kate Hansen (7TM-Pharma), and all mutations were done by site-directed mutagenesis using the *Pfu* polymerase (Stratagene, La Jolla, CA). The mutations were verified by DNA sequencing on an ABI 310 sequencer from Applied Biosystems (Foster City, CA).

Transfections and Tissue Culture. COS-7 cells were grown at 10% CO_2 and 37°C in Dulbecco's modified Eagle's medium with GlutaMAX (Invitrogen, Carlsbad, CA) adjusted with 10% fetal bovine serum, 180 U/ml penicillin, and 45 μg/ml streptomycin (Pen-Strep). Transfection of the COS-7 cells was performed by the calcium phosphate precipitation method (Rosenkilde et al., 1999). L1.2 cells stably expressing CCR8 (human or murine) were grown in 5% CO_2 and 37°C in RPMI 1640-based medium supplemented with 10% fetal

[1] In the text, we use the generic 7TM numbering system suggested by Baldwin (1993), and later modified by Schwartz (1994), whereas we include in the tables the nomenclature suggested by Ballesteros and Weinstein (1995).

bovine serum, 180 U/ml penicillin, and 45 μg/ml streptomycin (Pen-Strep). The density of the cell suspension was maintained around 0.7 to 1.0 million cells per milliliter. Cells were removed from the culture after approximately 2 months and replaced with freshly thawed cells of lower passage number.

Inositol Phosphate Accumulation. COS-7 cells were transfected according to the procedure mentioned above. In brief, 6×10^6 cells were transfected with receptor or vector control cDNA (from 20 μg/flask) together with 30 μg of the promiscuous chimeric G-protein Gqi4myr, which turns the $G\alpha_i$ coupled signal into the $G\alpha_q$ pathway (phospholipase C activation measured as IP accumulation) (Kostenis, 2001) One day after transfection, COS-7 cells (1.5×10^4 cells/well) were incubated for 24 h with 2 μCi of [*myo*-^{3}H]inositol in 0.4 ml of growth medium per well. Cells were washed twice in 20 mM HEPES, pH 7.4, supplemented with 140 mM NaCl, 5 mM KCl, 1 mM $MgSO_4$, 1 mM $CaCl_2$, 10 mM glucose, and 0.05% (w/v) bovine serum albumin and were incubated in 0.4 ml of buffer supplemented with 10 mM LiCl for 15 min. The ligands were subsequently added and incubated for 90 min. During the antagonist test, the LMD-009 compound was given 15 min before the endogenous agonist to ensure proper interaction of the receptors with LMD-009. Cells were extracted by addition of 1 ml of 10 mM formic acid to each well followed by incubation on ice for 30 to 60 min. The generated [^{3}H]inositol phosphates were purified on AG 1-X8 anion exchange resin. Determinations were made in duplicate.

Competition Binding Experiments. L1.2 cells stably expressing human CCR8 or murine CCR8 were split to 5×10^5/ml the day before the binding experiments. *N*-Butyric acid was added into the cell suspension (1:100 dilution) to a final concentration of 5 mM in the late afternoon. On the next day, the cells were harvested by 5 min of spinning (1350 rpm) and washed once with binding buffer (1× Hanks' balanced salt solution without phenol red, 0.1% bovine serum albumin, 0.02% NaN_3), followed by a resuspension in binding buffer at 2×10^6 cells/ml. The L1.2-CCR8 cell suspension (50 μl) was added into each well of the compound plate (10^5 cells/well) and pipetted up and down three times to mix. The unlabeled ligands were in the range from 0.1 nM to 100 μM, and 100 nM unlabeled CCL1 was used as a background control. The cells were incubated with the compounds for 40 min at room temperature. ^{125}I-CCL1 (50 μl; 0.2 nM) was added to each well and incubated at room temperature for 1 h. 100 μl of 0.33% polyethylenimine solution was added into each well of a filter plate (GF/B), and incubated for approximately 30 min at room temperature. The samples were harvested using a cell harvester (PerkinElmer Life and Analytical Sciences, Waltham MA), the plates were washed with four wells of ice-cold assay wash buffer, the harvester was opened, and the plate was dried under vacuum for approximately 30 s. The filter plate was then air-dried overnight, the plates were bottom-sealed, 500 μl of MicroScint-20 fluid (PerkinElmer Life and Analytical Sciences) was added to each well, the top of the plate was sealed using Topseal (PerkinElmer), and the plate was read on a Topcounter (PerkinElmer). Determinations were made in quadruplicates

Chemotaxis Experiments. The stably transfected L1.2 cells were grown overnight at 0.7 to 1×10^6 cells/ml in fresh media. The cells were counted and centrifuged at low speed (~1200 rpm) and resuspended in an equal volume of warm chemotaxis buffer (RPMI 1640 medium containing 0.5% bovine serum albumin), centrifuged again, aspirated, and re-suspended at 1.0×10^7 ells/ml in warm chemotaxis buffer. Chemotaxis was measured using 24 Transwell Polycarbonate 3 μm Membranes (Costar; Corning Life Sciences, Acton, MA). The bottom wells were filled with increasing concentrations of LMD-009 or CCL1 diluted in 0.6 ml of chemotaxis buffer. Chemotaxis plates were then incubated for 4 h at 37°C in a 5% CO_2-humidified incubator. After incubation, the cells from the bottom well were collected and counted manually or by a fluorescence-activated cell sorting (FACSCalibur; BD Biosciences, San Jose, CA). Samples were assayed in duplicate.

FLIPR-Calcium Mobilization Assay. Chinese hamster ovary/Gα16 cells stably expressing human CCR8 were plated on 384-well plates (Falcon; BD Biosciences Discovery Labware, Bedford, MA) at a density of 4×10^3 cells/well and cultured for 2 days at 37°C and 5% CO_2. On the third day, the cells were incubated with Fluo-3TM (5 μM) for 1 h (37°C, 5% CO_2), and excess dye was removed by extensively washing the cells. To measure the potency of CCR8 agonists to induce intracellular Ca^{2+}, plates were loaded onto a fluorometric imaging plate reader (FLIPR2; Molecular Devices Inc., Sunnyvale, CA). Ca^{2+} flux was induced by adding increasing amounts of CCL1, LMD-009, or dimethyl sulfoxide only (negative control). EC_{50} values were calculated using XLfit 4.0 (IDBS, Guildford, Surrey, UK).

Surface Enzyme-Linked Immunosorbent Assay. COS-7 cells were transiently transfected with the N-terminal FLAG-tagged variants of CCR8. The cells were washed once in TBS (50 mM Tris base and 150 mM NaCl, pH 7.6), fixed in 4% glutaraldehyde for 15 min after three washes in TBS and incubation in blocking solution (2% bovine serum albumin in TBS) for 30 min at room temperature. The cells were subsequently incubated for 2 h with anti-FLAG (M1) antibody (2 μg/ml) in TBS supplemented with 1% bovine serum albumin and 1 mM $CaCl_2$ at room temperature. After three washes in TBS with 1 mM $CaCl_2$ the cells were incubated with goat anti-mouse horseradish peroxidase-conjugated antibody in the same buffer as the anti-FLAG antibody for 1 h. After three washes in TBS supplemented with 1 mM $CaCl_2$, the immune reactivity was revealed by the addition of horseradish peroxidase substrate according to manufacturer's instructions.

Molecular Modeling. A model of the transmembrane helical bundle of the CCR8 receptor was created using SWISS-MODEL GPCR mode (http://swissmodel.expasy.org/cgi-bin/sm-gpcr.cgi; Schwede et al., 2003). To explore the energy landscape of LMD-009 and find the lowest energy conformation, a simulated annealing of LMD-009 was performed. This low-energy conformation of LMD-009 was manually docked into the binding pocket of CCR8 using the mutational study results. LMD-009 and the residues in close proximity of the ligand were subsequently minimized while ensuring that the initial conformation of the receptor or LMD-009 was not changed considerably.

Calculations. IC_{50} and EC_{50} values were determined by nonlinear regression by using Prism software (version 3.0; GraphPad Software, San Diego). K_i was calculated using the formula $K_i = IC_{50}$-[L], where [L] represents the concentration of applied radioligand.

Results

Identification of a Potent Nonpeptide CCR8 Receptor Agonist. In an effort to identify specific nonpeptide antagonists for CCR8, we identified an efficacious and potent CCR8 agonist, LMD-009 (Fig. 1). Comparison of the structure of LMD-009 with the recently disclosed CCR8 agonist ZK 756326 from Berlex Biosciences (Haskell et al., 2006) revealed structural similarity. However, LMD-009 activated human CCR8 with approximately 20-fold higher potency. In transiently transfected COS-7 cells expressing the human CCR8 receptor, we measured the ability of LMD-009 to stimulate inositol phosphate accumulation. This assay is based upon a cotransfection with the promiscuous Gqi4myr [a chimeric Gα-subunit that is identified as a $G\alpha_i$ subunit by the 7TM receptor but transduces a $G\alpha_q$ signal upon activation (Kostenis, 2001)]. Under these experimental settings, we observed a potency of LMD-009 that was rather similar to that of CCL1 [EC_{50} of 11 and 8.7 nM, respectively (Fig. 2A)]. Given that the artificial signaling experiments described above were dependent upon the presence of a chimeric promiscuous G-protein, we decided in addition to use more natural signaling pathways in other cell lines (i.e., lymphocyte

cell-line L1.2). We therefore tested the ability of LMD-009 to mediate calcium release in Chinese hamster ovary cells and to induce cell migration in the lymphocyte L1.2 cells. Consistent with the data observed from the IP accumulation assay (Fig. 2A), we observed the same efficacy for LMD-009 and CCL1 in the calcium release experiments (Fig. 2B) and in the chemotaxis experiments (Fig. 2C)—i.e., LMD-009 is a full agonist. In the calcium release experiments, we observed a potency (EC_{50}) of 87 ± 17 nM and a Hill coefficient of 1.39 ± 0.15 for LMD-009 (Fig. 2B).

Many nonpeptide antagonists in the chemokine system act as allosteric ligands with respect to showing low affinity in competition binding experiments (see, for instance, Watson et al., 2005; Rosenkilde and Schwartz, 2006). However, in stably transfected L1.2 cells, we observed an affinity (K_i) of 66 nM for LMD-009 and a complete displacement of all specifically bound ^{125}I-CCL1 (Fig. 2D). That is, the observed binding affinity for LMD-009 is comparable with its potency (Fig. 2).

LMD-009 Activates Only CCR8 Among Human Chemokine Receptors. All the generally accepted human CC, CXC, XC, and CX3C receptors were screened to probe the specificity of the LMD-009 compound. Thus, by measuring IP accumulation in transiently transfected COS-7 cells (cotransfected with Gqi4myr as above), we observed that the high potency of LMD-009 for human CCR8 was in fact highly selective, in that we did not observe any high-potency activation for any of the 17 tested endogenous chemokine receptors. In fact, we did not observe any activation by LMD-009 at concentrations up to 1 μM for CCR2–10, CXCR1–6, and CX3CR1, whereas CCR1 and XCR1 were activated to a slight degree at 1 μM. For all tested receptors, the effect of the endogenous ligand is shown as a positive control (Fig. 3). We also included CCR11 in our test and observed no activation by LMD-009, yet because no agonist has been identified for this receptor, we excluded it from Fig. 3. The recently deorphanized CXCR7 receptor (previously called RDC-1) was also tested; again, no activation by LMD-009 was observed. Yet because we could detect no activation with the proposed endogenous ligands for CXCR7 (CXCL11 and CXCL12), we have also excluded this receptor from Fig. 3. Interspecies variations in activity of nonpeptide ligands are critical for the valid analysis of these compounds in animal models. In particular, the activity of compounds on the murine homologs is important because of the many murine models of inflammation. We therefore tested the activity of LMD-009 in L1.2 cells stably expressing mouse CCR8 and observed a dose-dependent activation with the same efficacy as TCA-3 (the murine homolog of CCL1), albeit with an 8.5- and 15-fold lower potency [i.e., EC_{50} values of 740 and 580 nM for calcium release and chemotaxis, respectively (data not shown)]. A similar interspecies difference was found for the recently published ZK 756326, which acted with a 10-fold lower potency on murine CCR8 than on human CCR8 (Haskell et al., 2006). Greater species selectivity (>100-fold between rodent and nonrodent receptors) has been observed for other CC and CXC-receptor nonpeptide compounds such as the CCR1 antagonist BX471 (Horuk et al., 2001).

Molecular Interaction of LMD-009 with CCR8. GluVII:06 is an anchor point also for nonpeptide agonists. Nonpeptide antagonists against CC-chemokine receptors usually share a common pharmacophore with a rather centrally located, positively charged amine (Rosenkilde and Schwartz, 2006; Seibert et al., 2006). This amine has been shown to interact with a highly conserved Glu in the extracellular end of TM-VII (in position VII:06), whereas the flanking groups have been shown to interact with conserved aromatic residues, as well as other residues specific for each chemokine receptor (Mirzadegan et al., 2000; Castonguay et al., 2003; Tsamis et al., 2003; de Mendonça et al., 2005; Maeda et al., 2006; Seibert et al., 2006). Thus, all CC-chemokine receptor nonpeptide antagonists with characterized binding modes interact with GluVII:06 [except for the recently characterized binding pocket of BX471 in CCR1 (Vaidehi et al., 2006)] in addition to aromatic residues in the major binding pocket (composed of TM-III, TM-IV, TM-V, TM-VI, and TM-VII) and in the minor binding pocket (composed of TM-I, TM-II, TM-III, and TM-VII) (Fig. 1) (Mirzadegan et al., 2000; Castonguay et al., 2003; Tsamis et al., 2003; de Mendonça et al., 2005; Maeda et al., 2006; Seibert et al., 2006). Like most chemokine receptor nonpeptide ligands, LMD-009 contains a positively charged amine (the piperidine-ring of the spiro system). We therefore tested the ability of LMD-009 to activate a mutant form of CCR8 in which GluVII:06 was substituted by Ala (E286A). In this mutation LMD-009 displayed a nearly 1000-fold decreased potency (Table 1, Fig. 4), whereas the endogenous chemokine CCL1 was unaffected. Thus, the nonpeptide agonist LMD-009 resembles the majority of CC-chemokine nonpeptide antagonists in requiring interaction with GluVII:06.

Position VII:06 is located in the passage between the major and minor binding pockets (Fig. 1). In this interface region between TM-III and TM-VII, we mutated three other residues in TM-VII: 1) HisVII:03 (His^{283}), located almost one helical turn above GluVII:06 facing toward the minor binding pocket; 2) SerVII:09 (Ser^{289}), located almost one helical turn

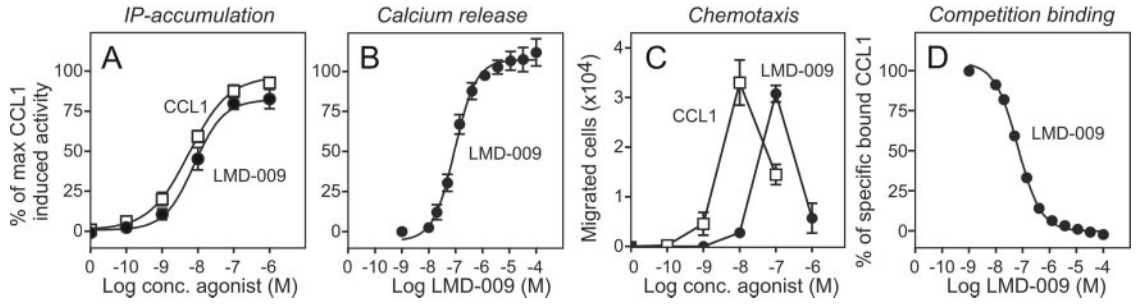

Fig. 2. LMD-009 activates CCR8 with high potency and efficacy and completely displaces ^{125}I-CCL1 with high affinity. A, the inositol phosphates (IP) accumulation experiments were performed in transiently transfected COS-7 cells. Dose-response curves with LMD-009 (□) and CCL1 (●). B and C, the calcium release experiments and the competition binding experiments were performed in stably transfected L1.2 cells. (n = 3–63).

below GluVII:06 facing toward the major binding pocket; and 3) PheVII:10 (Phe^{290}), located one helical turn below GluVII:06 (Fig. 1). We were surprised to find that, despite the close proximity to GluVII:06, Ala substitutions at these three positions had no impact on the binding of LMD-009 or CCL1 (Table 1). In TM-III, ValIII:04 (Val^{109}) is located in close proximity to GluVII:06, yet we observed no change in the potency of LMD-009 or CCL1 upon substitution of ValIII:04 to Ala (Table 1).

Aromatic Residues in Both the Minor and the Major Ligand-Binding Pockets Are Important for the Action of LMD-009. Several aromatic residues located at positions in the minor and major ligand-binding pocket, which previously have been described as "hits" (i.e., residues of importance) for nonpeptide antagonist targeting the CCR1, CCR2, and CCR5 receptors, were also identified as "hits" for the nonpeptide CCR8 agonist. Thus, in the minor binding pocket, the Ala substitution of TyrI:07 (Tyr^{42}) resulted in a 15-fold decrease in potency for LMD-009, whereas CCL1 was unaffected (Table 1). Likewise, Ala substitution of PheII:17 (Phe^{88}) resulted in a 10-fold decrease in potency for LMD-009, again with no effect on CCL1 (Table 1). In contrast, PheII:13 (Phe^{84}), one helical turn below PheII:17, had no impact on the interaction of LMD-009 or CCL1 with CCR8 (Table 1). The Gln residue at position II:20 (Gln^{81}) is unique for CCR8 among chemokine receptors (85% of endogenous chemokine receptors have a Trp in this position). We substituted Gln with Trp (Q91W) to induce steric hindrance and to make CCR8 more similar to the other CC-chemokine receptors. In contrast to the dependence for a Trp in position II:20 observed for CCR5 nonpeptide antagonists (Maeda et al., 2006; Seibert et al., 2006), we observed that both LMD-009 and CCL1 required a small and nonaromatic residue at this position. Thus, the potencies of LMD-009 and CCL1 were decreased by 10- and 7.9-fold, respectively, for the Q91W substitution (Table 1, Fig. 6). Not all aromatic residues in this minor pocket were important for the binding of LMD-009, because we observed an unchanged high potency for LMD-009 and for CCL1 for the Phe III:07 (Phe^{112})-to-Ala and the PheIII:18 (Phe^{123})-to-Ala substitutions. These positions both face more toward TM-II than toward the minor binding pocket and are both located relatively deep, which could explain the lack of involvement.

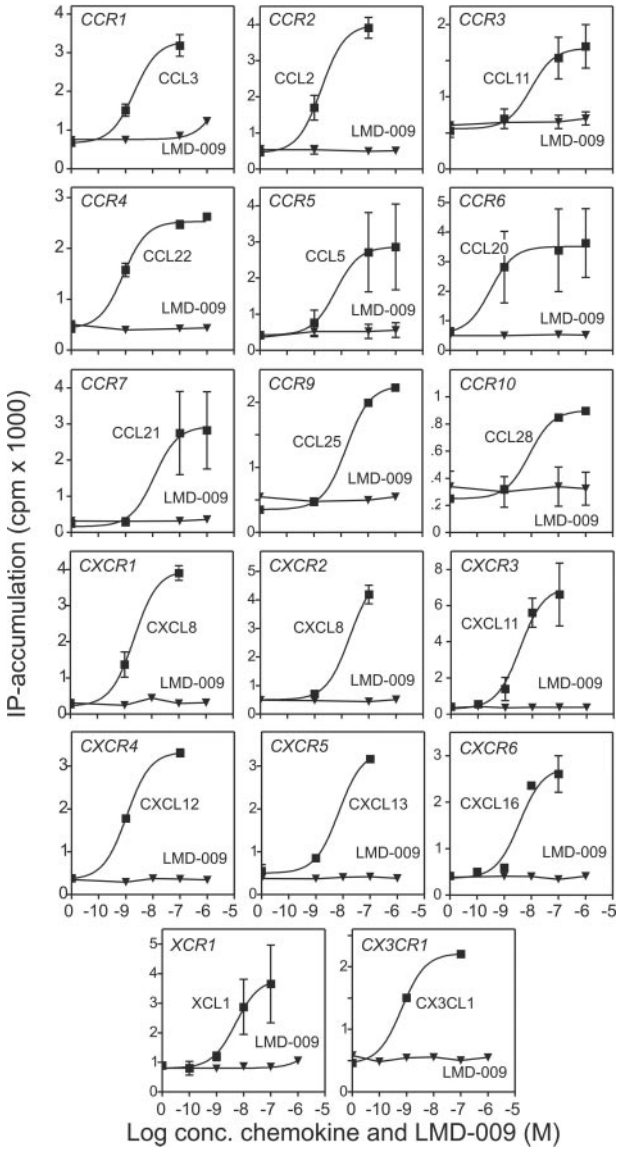

Fig. 3. Only LMD-009 activates CCR8 among all human chemokine receptors. The IP accumulation experiments were performed in transiently transfected COS-7 cells. Dose-response curves for LMD-009 (▼) and of the positive controls (■) selected among the possible endogenous chemokine agonists. (n = 3–63).

In the *major* binding pocket, we found that the highly conserved TyrIII:08 (Tyr^{113}) was essential for the action of LMD-009 in that a decrease in potency of nearly 1000-fold was observed for the Y113A substitution and that CCL1 was affected by this mutation with a 37-fold decrease in potency (Table 1, Fig. 5). This was not surprising, because this position is involved in the action of most CCR1, -2, and -5 nonpeptide antagonists as well (see *Discussion*). TM-VI contains two highly conserved aromatic residues: TrpVI:13 (Trp^{251})—part of the conserved "CWLP"-motif (Schwartz et al., 2006)—and PheVI:16 (Phe^{254}). We found that the TrpVI:13 was replaceable for the high potency of both LMD-009 and CCL1 based on two different substitutions —W251A and W251Q (Table 1, Figs. 5 and 6). The W251Q substitution was created because some chemokine receptors (CCR6, -7, -9, -11, and CXCR6) have a Gln instead of the otherwise highly conserved Trp in this position (see *Discussion*). The PheVI:16, which is located one helical turn above TrpVI:13, revealed a highly surprising phenotype upon substitution to Ala (F254A), with a 19-fold improvement of LMD-009 potency combined with an increase in the efficacy for the nonpeptide agonist relative to the endogenous CCL1 chemokine (Fig. 5). Thus, LMD-009 acted as a superagonist on the [F254A] mutant form of CCR8. In contrast, CCL1 displayed a 13-fold decrease in potency. One and two helical turns above PheVI:16, we substituted the LeuVI:20 (Leu^{258}) and SerVI:24 (Ser^{262}) with Ala —L258A and S262A, respectively. Both of these residues – like TrpVI:13 and PheVI:16 – face toward the major binding pocket. However, we did not observe any changes in the potency and efficacy of LMD-009 and CCL1 for the L258A and S262A mutations (Table 1, Fig. 6). Thus, in the major binding pocket only, TyrIII:08 was a classic mutational hit for the LMD-009–mediated activation of CCR8. But the almost 20-fold gain of function with respect to potency for LMD-009 observed upon Ala substitution of PheVI:16 indicates a close proximity of part of the nonpeptide to this

TABLE 1

Molecular interaction of CCL1 and LMD-009 with CCR8

The whole panel of CCR8 mutations was screened for the ability of the endogenous chemokine CCL1 (left) and the nonpeptide LMD-009 (right) to activate every single mutation. The CCR8 receptors were expressed in transiently transfected COS-7 cells, and the activation was measured by means of accumulated inositol phosphates (see *Materials and Methods*). The table shows the potency (both as Log EC_{50} and as EC_{50}) and the level of activation [basal and agonist stimulated levels (efficacy)]. The differences between the potency of CCL1 or LMD-009 on a given mutation and the potency of each ligand on wt CCR8 are shown in the columns named "-Fold." The number of experiments is given as n. The receptor residues are given according to the Schwartz (S) and Ballesteros/Weinstein (B-W) nomenclatures (see footnote 1 in the text.)

Residue			CCL1						LMD−009				
			Potency						Potency				
Position		Number	EC_{50}	EC_{50}	-Fold	n	Efficacy (E_{max})	Basal Activity	EC_{50}	EC_{50}	-Fold	n	Efficacy (E_{max})
S	B-W												
			Log	*nM*			*cpm*	*cpm*	*Log*	*nM*			*cpm*
wt	wt	wt	−8.1 ± 0.03	8.7	1.0	65	4000 ± 314	712 ± 40	−8.0 ± 0.17	11	1.0	11	3774 ± 448
I:07	1.39	Y42A	−7.9 ± 0.13	11	1.3	9	2238 ± 370	786 ± 120	−6.8 ± 0.09	158	15	3	1471 ± 302
I:11	1.43	F46A											
II:13	2.53	F84A	−8.4 ± 0.13	4.0	0.46	8	2098 ± 278	1009 ± 87	−7.9 ± 0.09	14	1.3	3	1441 ± 158
II:17	2.57	F88A	−8.0 ± 0.05	10	1.2	9	2445 ± 419	799 ± 118	−7.0 ± 0.05	108	10	4	1107 ± 450
II:20	2.60	Q91W	−7.2 ± 0.14	69	7.9	6	1232 ± 101	665 ± 58	−7.0 ± 0.18	108	10	3	2916 ± 92
III:04	3.28	V109A	−8.1 ± 0.07	8.2	0.95	3	2100 ± 356	940 ± 269	−8.1 ± 0.21	7.7	0.73	3	2193 ± 297
III:05	3.29	S110A	−8.8 ± 0.10	1.6	0.18	8	2804 ± 723	861 ± 214	−8.8 ± 0.41	1.5	0.14	4	1066 ± 596
III:05	3.29	S110H	<−6	>1000	>137	7	N.E.	556 ± 850	<−5	>10,000	>950	2	N.E.
III:05	3.29	S110W	<−6	>1000	>137	5	N.E.	400 ± 108	<−5	>10,000	>950	2	N.E.
III:07	3.31	F112A	−8.3 ± 0.07	4.6	0.53	9	3706 ± 552	651 ± 88	−7.9 ± 0.04	11	1.1	4	2394 ± 702
III:08	3.32	Y113A	−6.5 ± 0.12	323	37	10	1047 ± 185	570 ± 57	<−5 ± 0.00	>10,000	>950	5	N.E.
III:09	3.33	Y114A	−6.9 ± 0.13	131	15	4	2692 ± 784	927 ± 200	−7.4 ± 0.09	42	3.9	6	3652 ± 710
III:18	3.42	F123A	−8.4 ± 0.15	4.4	0.51	6	1466 ± 371	426 ± 64	−8.2 ± 0.14	7.0	0.66	3	1430
IV:20	4.60	L168D	−7.9 ± 0.18	12	1.4	11	3549 ± 537	948 ± 122	−7.8 ± 0.17	18	1.7	2	4410 ± 1576
IV:24	4.64	Y172A	−8.0 ± 0.11	11	1.3	8	2000 ± 155	1315 ± 110	−7.7 ± 0.15	21	2.0	4	1557 ± 329
V:−02	5.33	K193A	−7.7 ± 0.17	22	2.6	6	2956 ± 352	659 ± 89	−8.1 ± 0.37	8.5	0.80	2	3414 ± 298
V:−01	5.34	W194A	−6.9 ± 0.29	128	15	5	2500 ± 142	673 ± 44	−8.1 ± 0.23	7.6	0.72	3	1273 ± 207
V:01	5.35	K195A	−8.1 ± 0.09	7.5	0.87	7	1947 ± 314	666 ± 97	−8.2 ± 0.30	6.2	0.59	3	2370 ± 485
V:12	5.46	G206A	−7.2 ± 0.13	67	7.7	9	904 ± 63	508 ± 54	−7.7 ± 0.08	19	1.4	3	744 ± 59
V:12	5.46	G206W	N.A.			8	501 ± 75	N.A.	N.A.			3	
VI:13	6.48	W251Q	8.5 ± 0.12	3.4	0.39	10	2245 ± 347	1146 ± 152	−7.8 ± 0.34	44	4.1	3	1112 ± 468
VI:13	6.48	W251Q	−8.2 ± 0.14	6.6	0.76	6	2528 ± 320	1097 ± 166	−7.4 ± 0.34	44	4.1	3	1112 ± 468
VI:16	6.51	F254A	−7.0 ± 0.09	109	13	10	3131 ± 609	835 ± 74	−9.2 ± 0.24	0.57	0.05	5	6640 ± 1484
VI:20	6.55	L258A	−7.6 ± 0.11	27	3.2	9	2699 ± 262	591 ± 54	−7.9 ± 0.20	13	1.2	3	3162 ± 568
VI:24	6.59	S262A	−8.3 ± 0.10	5.2	0.60	10	2949 ± 420	621 ± 67	−7.7 ± 0.16	21	2.0	4	1854 ± 815
VII:03	7.36	H283A	−7.9 ± 0.09	12	1.4	8	4003 ± 444	705 ± 58	−7.6 ± 0.14	24	2.2	3	3644 ± 1595
VII:06	7.39	E286A	−7.9 ± 0.11	12	1.4	11	3732 ± 578	930 ± 96	<−5	>10000	>950	5	N.E.
VII:09	7.42	S289A	−7.7 ± 0.14	18	2.1	3	9229 ± 3007	842 ± 293	−7.8 ± 0.03	16	1.5	3	10833 ± 2827
VII:10	7.43	F290A	−8.2 ± 0.20	6	0.68	5	4325 ± 940	2497 ± 517	−7.7 ± 0.08	20	1.9	5	3700 ± 789

N.E., not estimated due to no plateau; N.A., no activation at all.

position in CCR8. Both of these mutations impaired the action of CCL1 to the same extent.

Residues in TM-III, TM-IV, and TM-V Facing into the Major Binding Pocket. Most of these residues are more polar and nonaromatic, except for TyrIII:09 (Tyr^{114}) and TyrIV:24 (Tyr^{172}). A Tyr in position III:09 is also found in CCR1, where it was recently shown to be important for the binding of the nonpeptide antagonist BX471 (Vaidehi et al., 2006). However, we observed only a minor decrease in the potency of LMD-009 (3.9-fold) for the TyrIII:09 to Ala substitution, whereas the potency of CCL1 was decreased 15-fold (Table 1). Position IV:24 has been shown to be involved in the binding of aplaviroc to CCR5 (Maeda et al., 2006); however, we observed no change in the potency of LMD-009 or CCL1 for the Ala substitution in this position (Table 1). SerIII:05 (Ser^{110}) was changed to Ala, His, and Trp, and whereas the Ala substitution resulted in a slight increase (5–7-fold) in the potency of LMD-009 as well as CCL1, the steric hindrance approach severely impaired the activation by both agonists (Table 1). A basic residue is found in position V:01 in 50% of all chemokine receptors, and in CCR5, LysV:01 (Lys^{195}) has been shown to be important for the binding of aplaviroc (Maeda et al., 2006). This was not the case in CCR8, in that we observed no change in the potency of LMD-009 or CCL1 for the corresponding LysV:01 to Ala substitution (Table 1, Fig. 6). Because the tertiary structure of the extracellular end of TM-V is uncertain (Javitch et al., 2002; Rosenkilde et al., 2006), we mutated a couple of residues presumably located in the adjacent part of extracellular loop 2, Lys^{193} (position V:-02) and the Trp^{194} (in position V:-01). These substitutions had no effect on the potency of LMD-009, whereas CCL1 was impaired with a 15-fold decrease in potency for the W194A substitution (Table 1). Position V:12 contains a Gly in almost all chemokine receptors; however, substitution with Ala at this position (Gly^{206}) had no effect on the potency of LMD-009, whereas the potency of CCL1 was impaired by 7.7-fold. In contrast, a substitution with Trp in a steric hindrance approach totally abolished receptor activation by both agonists (Table 1), despite measurable receptor surface expression (Fig. 9B).

Binding Mode for Different LMD Compounds. Besides the LMD-009 compound, we included in the current study a series of four analogs that all differed from LMD-009 with regard to the left side. Thus, they all contained the methoxyphenoxybenzyl (right side) and the centrally located positively charged piperidine. The left sides were either relatively short with a benzoic acid (LMD-584) or a methoxybenzenesulfonamide (LMD-902) or amide-elongated with either a phenyl-4-(pyrrolidin-1-yl)butanamide (LMD-268) or a oxoquinoline-4-carboxamide (LMD-174) (Fig. 7). The four compounds were all probed to the same generated CCR8 mutation library as for LMD-009 using the same functional assay with stimulation of IP accumulation. It is noteworthy that only a very few mutations turned out to affect the

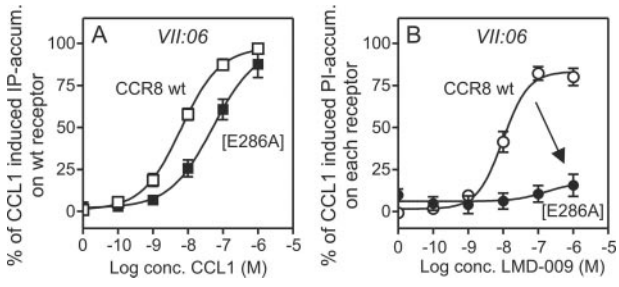

Fig. 4. GluVII:06 is an anchor-point for LMD-009. The IP accumulation experiments were performed in transiently transfected COS-7 cells. A, dose-response curves for CCL1 on CCR8 wt (□) and E286A (■), where 100% equals the maximal stimulation of CCL1 on CCR8 wt. B, dose-response curves for LMD-009 on CCR8 wt (○) and E286A (●), where 100% equals the maximal stimulation of CCL1 on each receptor. (n = 3–63).

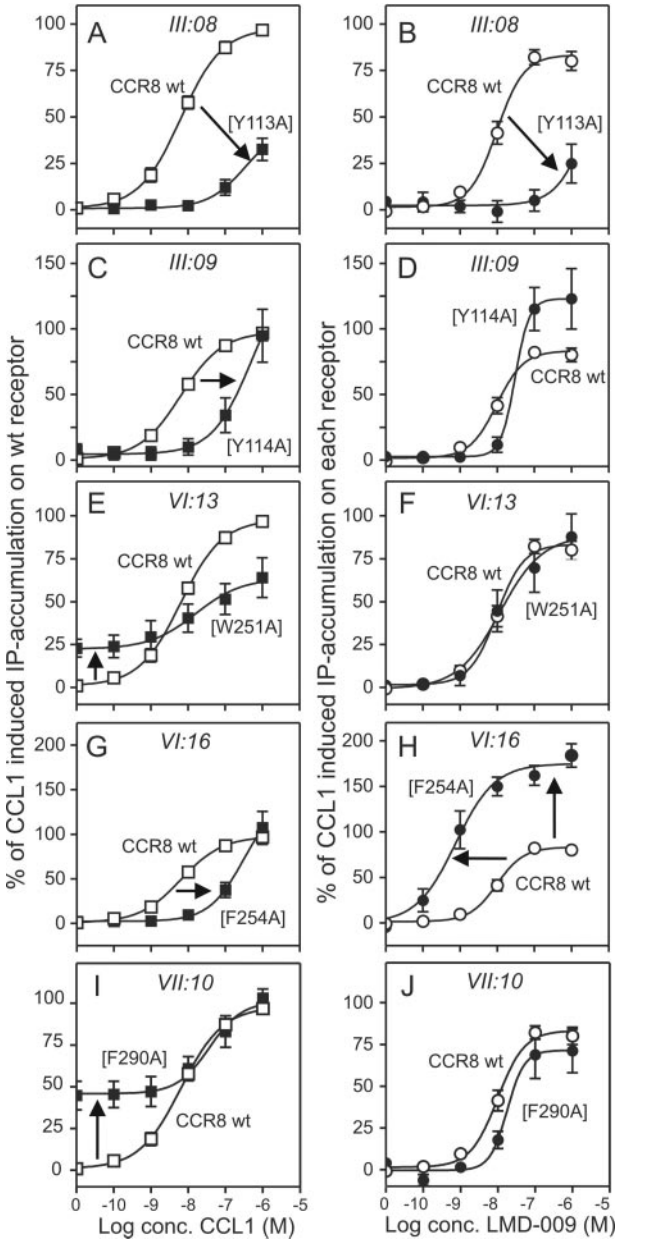

Fig. 5. CCL1 and LMD-009 depend upon certain aromatic residues in CCR8. The IP-accumulation experiments were performed in transiently transfected COS-7 cells. A selection of aromatic residues mutated into Ala is presented. CCL1: wt, □; mutated receptors, ■; LMD-009: wt, ○; mutated receptors, ●. A and B, mutation of TyrIII:08 to Ala (Y113A). C and D, mutation of TyrIII:09 to Ala (Y114A). E and F, mutation of TrpVI:13 to Ala (W251A). G and H, mutation of PheVI:16 to Ala (F254A). I and J, mutation of PheVII:10 to Ala (F290A). The curves for CCL1 (A, C, E, G, I) are all normalized to the basal and maximum IP accumulation on wt receptor, whereas the curves for LMD-009 (B, D, F, H, J) are all normalized to the basal and maximum CCL1 induced IP accumulation on each receptor. (n = 3–63).

nonpeptides differently (Fig. 7, Table 2). Thus, none of four analogs differed from LMD-009 with respect to receptor recognition in the minor binding pocket because they were all affected by the same mutations [i.e., Y42A (4.6- to 19-fold decrease in potency), F88A (3.1- to 14-fold decrease in potency), and Q91W (6.7- to 18-fold decrease in potency)]. In contrast, the mutations in the major binding pocket affected the compounds with a remarkable and more diverse pattern

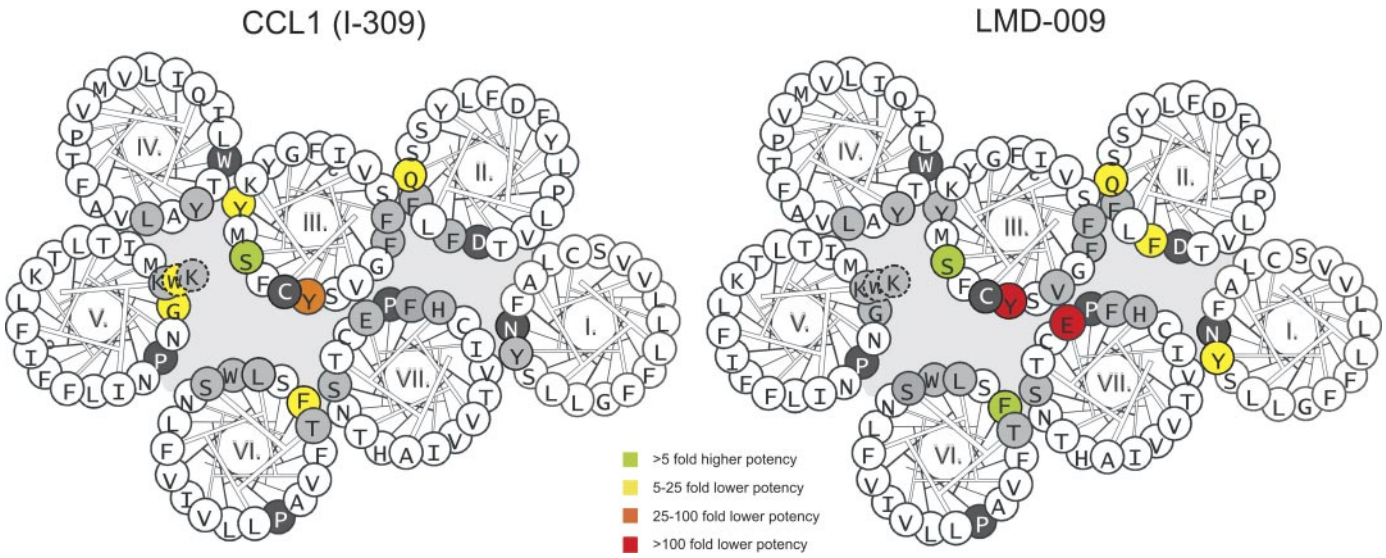

Fig. 6. Residues identified through mutagenesis to be important for the action of CCL1 and LMD-009 shown in a helical wheel diagram of the CCR8 receptor. The background colors indicate the magnitude of the effect of the mutation on the action of CCL1 (left) and LMD-009 (right). Grey background indicates <5-fold decrease in potency; yellow, 5- to 25-fold decrease; orange, 25- to 100-fold decrease, red, >100-fold decrease in potency. Green background indicates >5-fold increase in potency. The actual potencies are shown in Table 1.

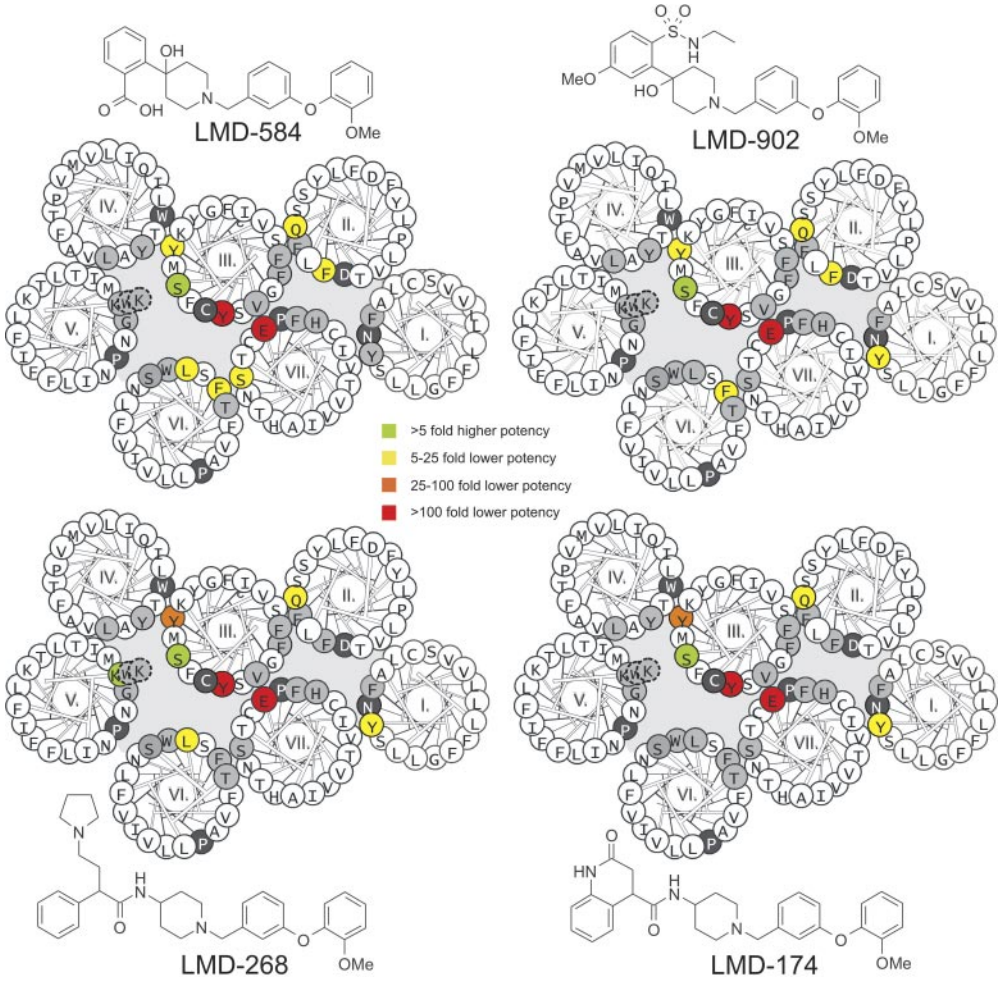

Fig. 7. Residues identified through mutagenesis to be important for the action of LMD-584, LMD-268, LMD-902, and LMD-174 shown in a helical wheel diagram of the CCR8 receptor. The background colors indicate the magnitude of the effect of the mutation on the action of LMD-584 , LMD-902, LMD-268, and LMD-174 . Grey background indicates <5-fold decrease in potency; yellow, 5- to 25-fold decrease; orange, 25- to 100-fold decrease; red, >100-fold decrease in potency. Green background indicates >5-fold increase in potency. The actual potencies are shown in Table 2.

TABLE 2

Molecular interaction of LMD-584, LMD-902, LMD-268, and LMD-174 with CCR8

The whole panel of CCR8 mutations was screened for the ability of the four additional nonpeptide agonists to activate every single mutation. The CCR8 receptors were expressed in transiently transfected COS-7 cells, and the activation was measured by means of accumulated inositol phosphates. The table shows the potency (both as Log EC_{50} and as EC_{50}). The differences between the potency of each compound on a given mutation and the potency of each ligand on wt CCR8 are shown in the columns named "-Fold." The number of experiments is given as *n*. The receptor residues are given according to the Schwartz (S) and Ballesteros/Weinstein (B-W) nomenclatures (see footnote 1 in the text).

Residue			LMD−584				LMD−902				LMD−268				LMD−174			
Position		Number																
S	B-W		EC_{50}	EC_{50}	-Fold	n	EC_{50}	EC_{50}	-Fold	n	EC_{50}	EC_{50}	-Fold	n	EC_{50}	EC_{50}	-Fold	n
			Log	*nM*			*Log*	*nM*			*Log*	*nM*			*Log*	*nM*		
wt	wt		−7.5 ± 0.07	29	1.0	15	−7.8 ± 0.10	15	1.0	8	−8.0 ± 0.05	9.0	1.0	4	−7.5 ± 0.05	30	1.0	15
I:07	1.39	Y42A	−6.9 ± 0.04	131	4.6	3	−6.7 ± 0.18	178	12	3	−6.8 ± 0.22	172	19	3	−6.7 ± 0.14	199	6.6	3
I:11	1.43	F46A	−6.9 ± 0.05	126	4.4	3	−7.3 ± 0.07	50	3.4	3	−7.4 ± 0.06	43	4.8	2	−7.3 ± 0.18	52	1.7	3
II:13	2.53	F84A	−8.2 ± 0.25	7.0	0.24	4	−7.9 ± 0.03	12	0.85	3	−8.3 ± 0.06	4.8	0.54	4	−6.9 ± 0.28	133	4.4	4
II:17	2.57	F88A	−6.6 ± 0.19	251	8.8	3	−6.7 ± 0.20	197	14	4	−7.5 ± 0.23	31	3.5	3	−7.0 ± 0.05	94	3.1	3
II:20	2.60	Q91W	−6.4 ± 0.36	368	13	3	−6.7 ± 0.13	180	12	3	−6.8 ± 0.25	161	18	3	−6.7 ± 0.17	201	6.7	3
III:04	3.28	V109A	−7.5 ± 0.26	34	1.2	3	−8.1 ± 0.05	8	0.52	3	−8.6 ± 0.11	2.6	0.29	3	−7.5 ± 0.18	33	1.1	3
III:05	3.29	S110A	−8.2 ± 0.38	6.0	0.21	4	−8.7 ± 0.34	2	0.15	3	−8.8 ± 0.11	1.6	0.18	6	−8.4 ± 0.15	3.6	0.12	4
III:05	3.29	S110H	<−5	>10,000	>323	3	<−5 ± 0.00	>10,000	>689	2	<−5	>10,000	>1100	2	<−5	>10,000	>323	3
III:05	3.29	S110W	<−5	>10,000	>323	4	<−5 ± 0.00	>10,000	>689	2	<−5	>10,000	>1100	3	<−5	>10,000	>323	3
III:07	3.31	F112A	−7.3 ± 0.08	51	1.8	4	−7.9 ± 0.09	13	0.88	4	−8.1 ± 0.08	7.1	0.79	6	−7.4 ± 0.08	37	1.2	4
III:08	3.32	Y113A	<−5 ± 0.00	>10,000	>323	3	>−5	>10,000	>689	3	<−5	>10,000	>1100	3	<−5 ±	>10,000	>332	3
III:09	3.33	Y114A	−6.4 ± 0.32	430	15	3	−6.7 ± 0.11	191	13	3	−6.2 ± 0.06	579	64	3	−6.0 ± 0.11	945	31	3
III:18	3.42	F123A	−7.7 ± 0.14	21	0.73	3	−7.9 ± 0.02	12	0.85	3	−8.3 ± 0.17	5.0	0.56	5	−7.7 ± 0.07	19	0.63	3
IV:24	4.64	Y172A	−7.3 ± 0.19	56	1.9	4	−7.5 ± 0.15	31	2.1	3	−7.6 ± 0.20	28	3.1	3	−7.0 ± 0.04	93	3.1	5
V:−02	5.34	K193A	−7.5 ± 0.18	31	1.1	4	−7.8 ± 0.52	17	1.2	2	−8.3 ± 0.17	4.7	0.52	3	−7.5 ± 0.06	30	1.0	3
V:−01	5.33	W194A	−7.9 ± 0.15	12	0.44	4	−8.4 ± 0.40	4	0.29	3	−8.2 ± 0.18	6	0.71	3	−7.5 ± 0.11	32	1.1	3
V:01	5.35	K195A	−7.7 ± 0.17	20	0.70	5	−8.2 ± 0.25	7	0.48	3	−9.7 ± 0.20	0.22	0.02	2	−7.5 ± 0.05	30	1.0	4
V:12	5.46	G206A	−7.3 ± 0.21	47	1.6	3	−7.9 ± 0.04	12	0.83	3	−8.8 0.10	2	0.19	2	−7.20.5	62	2.1	3
V:12	5.46	G206W	N.A.			3	N.A.			3	N.A.			3				3
VI:13	6.48	W251A	−7.7 ± 0.38	20	0.70	3	−8.30.14	4.7	0.32	2	−7.4 ± 0.25	42	4.7	4	−7.5 ± 0.41	29	0.97	3
VI:13	6.48	W251Q	−7.7 ± 0.41	22	0.77	3	−7.80.14	15	1.0	2	−8.0 ± 0.39	10	1.1	3	−7.5 ± 0.41	29	0.97	3
VI:16	6.51	F254A	−6.6 ± 0.19	278	9.7	4	−7.1 ± 0.04	80	5.5	3	−8.0 ± 0.12	10	1.2	3	−7.4 ± 0.13	42	1.4	3
VI:20	6.55	L258A	−6.5 ± 0.29	329	12	3	−7.5 ± 0.08	35	2.4	3	−7.2 ± 0.05	65	7.2	5	−7.2 ± 0.08	64	2.1	3
VI:24	6.59	S262A	−7.2 ± 0.13	61	2.1	3	−7.9 ± 0.10	13	0.86	3	−8.1 ± 0.28	8.9	1.0	5	−7.4 ± 0.02	39	1.3	3
VII:02	7.35	T282A	−7.1 ± 0.07	77	2.7	3	−7.5 ± 0.10	31	2.1	3	−7.4 ± 0.08	40	4.4	3	−7.0 ± 0.06	93	3.1	3
VII:03	7.36	H283A	−7.5 ± 0.08	30	1.0	3	−7.5 ± 0.06	34	2.4	3	−7.8 ± 0.11	17	1.9	3	−7.3 ± 0.09	46	1.5	3
VII:06	7.39	E286A	<−5	>10,000	>323	3	<−5	>10,000	>689	3	<−5	>10,000	>1100	5	<−5	>10,000	>332	3
VII:09	7.42	S289A	−6.7 ± 0.27	211	7.4	3	−7.5 ± 0.04	34	2.3	3	−7.8 ± 0.08	17	1.9	3	−7.4 ± 0.02	36	1.2	3
VII:10	7.43	F290A	−7.4 ± 0.24	41	1.4	3	−7.6 ± 0.31	26	1.8	3	−7.7 ± 0.34	21	2.3	4	−7.5 ± 0.46	29	1.0	3

N.A., no activation at all.

compared with LMD-009, although the dependence for TyrIII:08 was high, similar to that for LMD-009. Thus, the improved potency for LMD-009 in the PheVI:16 substitution to Ala (F254A) was not identified for any of the analogs, because the potencies of LMD-584 and LMD-902 were 9.7- and 5.5-fold impaired, respectively, whereas the two amide-elongated compounds were unaffected. The TyrIII:09-to-Ala substitution did not affect LMD-009 (Table 1); however, we observed impairment of all four analogs for Y114A. Thus, the potencies of LMD-584 and of LMD-902 were 15- and 13-fold impaired, whereas the potencies of the two amide-elongated compounds were even more impaired (64- and 31-fold decrease in potency for LMD-268 and LMD-009; Fig. 7). Two of the four compounds (LMD-584 and LMD-902) were also impaired by the Ala substitution of LeuVI:20, with a 12- and 7.2-fold decrease in potency; in addition, LMD-584 was affected by the SerVII.09 substitution to Ala with a 7.4-fold impaired potency. Thus, all these differences in the impact of the mutations in the major binding pocket clearly indicated that the left side of the compounds was located in this part of the main binding pocket and that the right side is located in the minor binding pocket with the GluVII:06/piperidine interaction as bridge.

Molecular Modeling of the Interaction of LMD-009 with CCR8. A model of the transmembrane helices of CCR8 was created based on an alignment with the bovine rhodopsin crystal structure (Palczewski et al., 2000). It is noteworthy that the residues identified by mutagenesis studies as being important for CCR8 activation by LMD-009 (Figs. 4–6 and Table 1) were all located at the same level in the receptor (Fig. 8A). A simulated annealing of LMD-009 was performed to explore the energy landscape of LMD-009 and to find the lowest energy conformation (data not shown). This low-energy conformation of LMD-009 was manually docked into the binding pocket in CCR8 identified by the mutagenesis studies using the presumed interaction of the positively charged amine with the negatively charged carboxylic group of GluVII:06 as a major docking point. LMD-009 and the residues

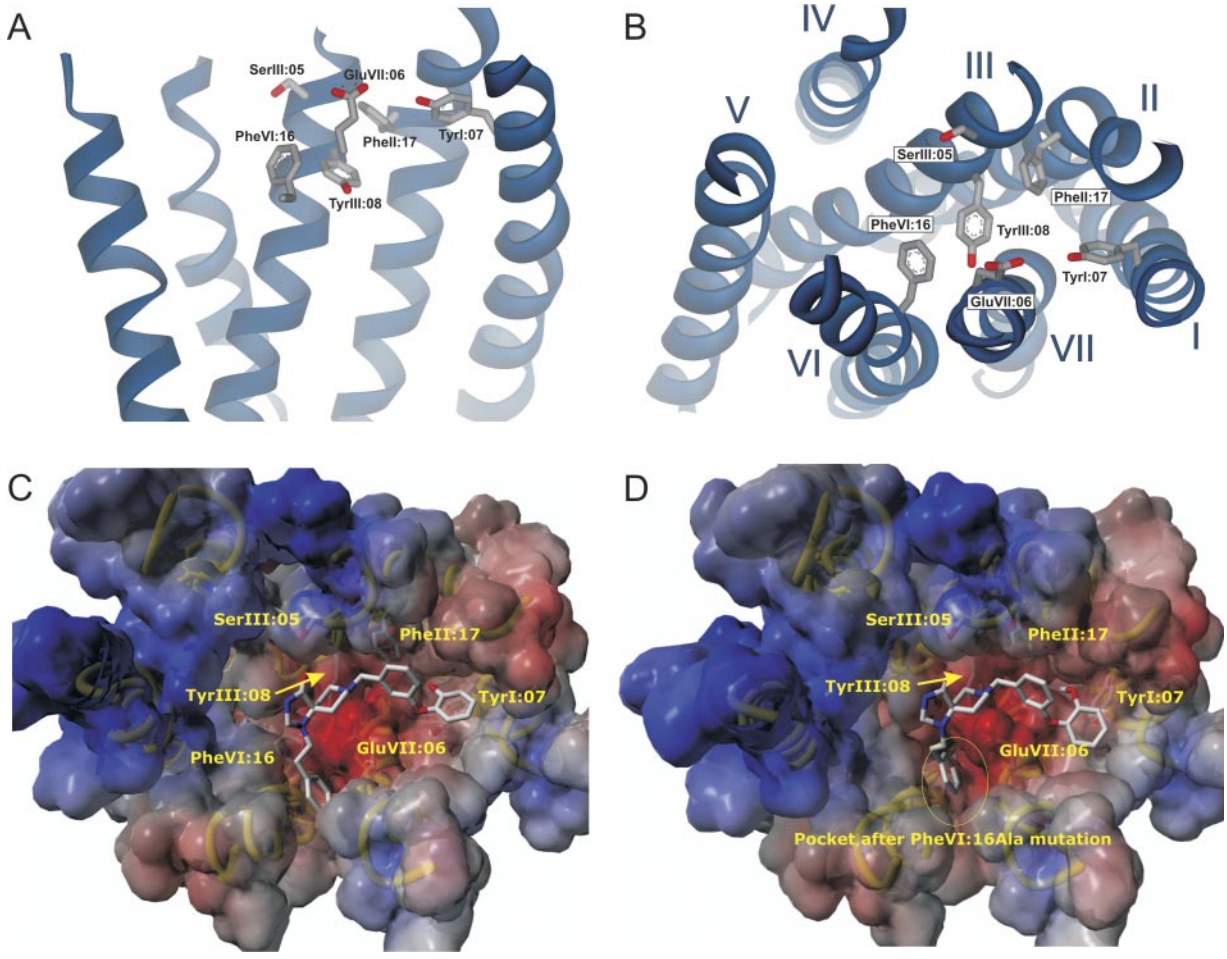

Fig. 8. Molecular model of the interaction of LMD-009 with the transmembrane helical bundle of the CCR8 receptor. The CCR8 model was built over the X-ray structure of bovine rhodopsin, and a low-energy conformation of LMD-009 was generated by simulated annealing (see text for details). A, side view of the helical bundle—shown in blue solid ribbons—of the CCR8 receptor with the residues identified by mutagenesis as presumed interaction points for LMD-009 (Fig. 5, Table 1) shown in stick models and where the ribbons for TM-VI and -VII have been removed in front for better view of the binding site. B, top view from the extracellular side of the model shown in A. C, top view of the CCR8 model with the electrostatic surface displayed (negative charge in red and positive charge in blue) where LMD-009—shown in stick model—has been docked into its presumed binding site. The electrostatic surfaces of the binding pocket is dominated by the negative charge of GluVII:06, which interacts with the positive charged nitrogen of the piperidine ring of LMD-009. The position of the side chains of the presumed contact residues are indicated by yellow labels. D, top view similar to that shown in C of a model of the F254A-CCR8 construct, which demonstrated a 19-fold gain of function for LMD-009. It is proposed that the phenethyl ring of the left side of LMD-009 as shown is able to insert into the pocket generated between TM-VI and TM-VII through the PheVI:16 to Ala substitution and that this improved fit could be responsible for the gain of function with respect to LMD-009 potency observed in the F254A-CCR8 construct.

near it were subsequently minimized while ensuring that the initial conformation of the receptor and LMD-009 was not changed considerably. Using this approach, LMD-009 could be positioned to make potential interactions with all the identified contact residues (Fig. 8) The methoxyphenoxybenzyl group (in the right side of LMD-009; Fig. 1) was positioned into the minor binding pocket (i.e., between TM-I, TM-II, TM-III, and TM-VII), with the two benzene rings having favorable hydrophobic interactions with TyrI:07 and PheII:17, respectively (Fig. 8C). The aromatic phenethylimidazoline-4-one (the left side of LMD-009) was placed in the major binding pocket (between TM-III, TM-VI, and TM-VIII) near Tyr III:08. The major gain of LMD-009 function for the PheVI:16 to Ala (F254A) mutation was further explored by construction of a computer model of the helical bundle of the F254A-CCR8 receptor (Fig. 8D). Using a similar docking approach as presented above—but allowing for further rotation of the phenethyl group at the left side of LMD-009—it was possible to dock this side-chain moiety of the nonpeptide agonist into the small, deep cavity, which was created between TM-VI and VII by the PheVI:16 to Ala mutation in the receptor (Fig. 8D). This "improved fit" docking of LMD-009 could potentially represent the structural basis for the observed gain-of-function for this compound in the PheVI:16-to-Ala mutation (Fig. 5H).

Receptor Expression versus Receptor Activity. Among the 29 mutations, we observed huge changes in basal and/or agonist-stimulated activity for some (Table 1, Fig. 9A). Thus, although some mutations resulted in large increases in basal (or agonist stimulated) activity, other resulted in the opposite. We therefore decided to N-terminally FLAG-tag a selection of these receptors chosen among the mutations with changed activity levels compared with CCR8 wt to determine receptor expression based on a surface ELISA (Fig. 9B). Mutations in four aromatic residues resulted in the largest increase in basal activity, with the Ala substitution of PheVII:10 (F290A) resulting in the highest constitutive activity, followed by the Ala substitution of TyrIV:24 (Y172A), the Ala/Gln substitutions of TrpVI:13 (W251A/Q), and the Ala substitution of PheII:13 (F84A). It is noteworthy that these increases were not followed by corresponding increases in the receptor expression levels (Fig. 9B). In contrast, the decreases in basal and agonist-stimulated activity for His/Trp substitution of SerIII:05 and of Ala/Trp substitution of GlyV:12 were in fact correlated with a remarkably lower surface expression. Among these four mutations, we could measure only the efficacy for G206A, because the agonist potencies for the three other mutations were decreased to an extent that prevented saturation (no plateau was reached in the dose-response curves; Table 1).

LMD-009 Is Not an Antagonist for Other Human Chemokine Receptors. Because of the similarities in the pharmacophore of LMD-009 to many CC-chemokine receptor antagonists (Mirzadegan et al., 2000; Castonguay et al., 2003; Tsamis et al., 2003; de Mendonça et al., 2005; Maeda et al., 2006; Rosenkilde and Schwartz, 2006; Seibert et al., 2006; Seibert et al., 2006) as described above, it was tempting to believe that LMD-009 would in fact act as an antagonist for other CC-chemokine (or maybe even CXC-chemokine) receptors. We therefore repeated the activity screen of LMD-009, this time as antagonist. Thus, the different receptors were activated with submaximal concentrations (from 40–80% stimulation) of the different respective endogenous chemokines, and the putative antagonistic properties of LMD-009 were tested with the results that none of the receptors were inhibited by LMD-009 (Fig. 10).

Discussion

In the present study, we identify a highly potent and selective CCR8 nonpeptide agonist, LMD-009, and describe its molecular interaction with CCR8 by combining receptor mutagenesis with studies of different chemical analogs of LMD-009. This is, to our knowledge, the first time the molecular interaction of a nonpeptide agonist with a chemokine receptor has been described. It is noteworthy that we show that the action of LMD-009 (and of the four analogs) depend upon several broadly distributed residues in common with known CC-chemokine receptor antagonists (e.g., the highly conserved GluVII:06 in the passage between the major and minor binding pocket, the TyrIII:08 in the major binding pocket, and the TyrI:07 and PheII:17 in the minor binding pocket).

Chemokine Receptor Interaction of Nonpeptide Antagonists versus Nonpeptide Agonists. From a structural point of view, the majority of small molecule nonpeptide ligands for CC-chemokine receptors are relatively elongated

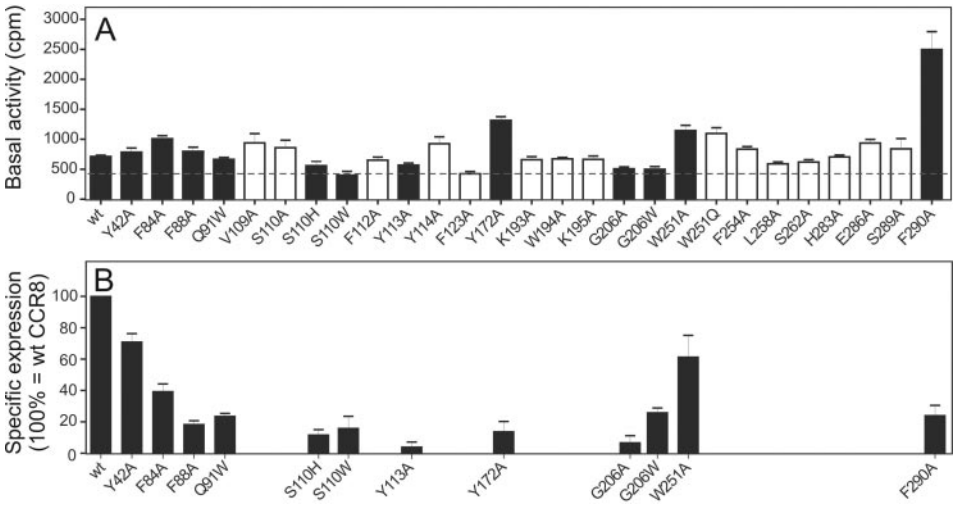

Fig. 9. Receptor activation and receptor expression levels. A, basal receptor activity measured by IP accumulation for all CCR8 mutations, adapted from Table 1. The mutations depicted in black columns were chosen for FLAG-tagging followed by surface expression determination (ELISA). B, the ELISA was performed in transiently transfected COS-7 cells using the same transfection method as for the activity measurements in (A); 100% equals the specific expression of wt CCR8. ($n = 3$).

structures characterized by one (or two) positively charged nitrogen atom(s) located more or less centrally in the molecule (Rosenkilde and Schwartz, 2006). Nonpeptide antagonists following this simplified "pharmacophore model" have almost all been shown to interact with the GluVII:06 via the positively charged nitrogen (Rosenkilde and Schwartz, 2006). However, an elegant study in CCR1 showed that the nonpeptide antagonist, BX471, was not dependent upon GluVII:06 but instead interacted with aromatic residues on each side of it, TyrI:07, TyrII:20 and TyrIII:09 (Vaidehi et al., 2006). GluVII:06 is conserved among chemokine receptors (found in 16 of 21 receptors) and occurs very rarely in nonchemokine receptors (Rosenkilde and Schwartz, 2006). In the present study, we describe how the nonpeptide agonist LMD-009 is dependent upon GluVII:06 in CCR8, presumably through a direct interaction of the spiro-ring with the piperidine and

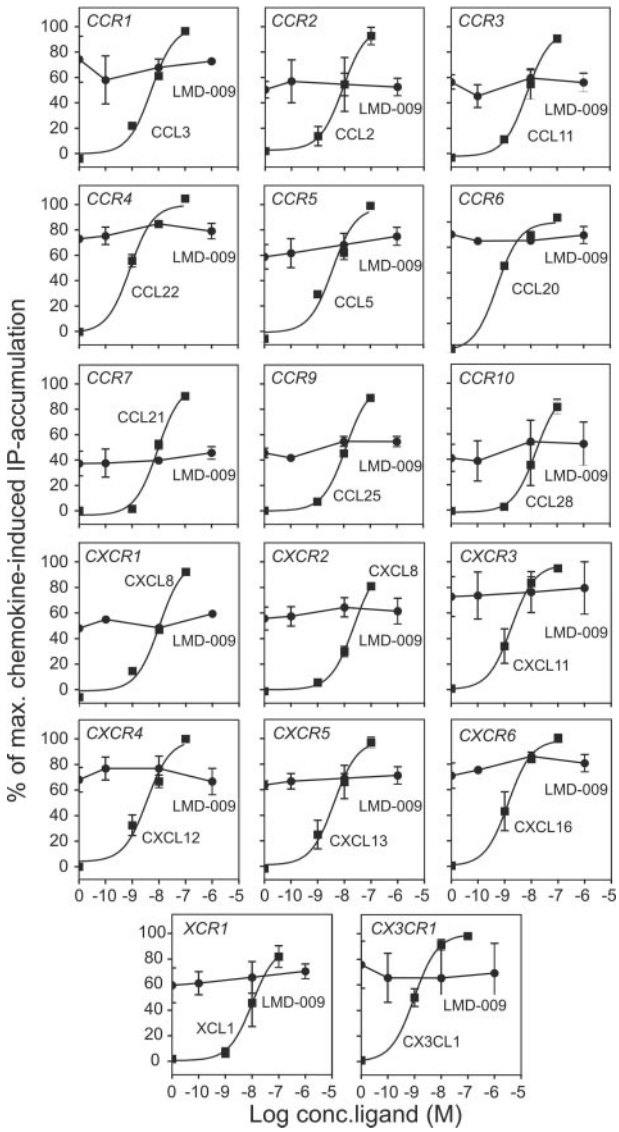

Fig. 10. LMD-009 is not an antagonist for any human chemokine receptor. The IP accumulation experiments were performed in transiently transfected COS-7 cells. Dose-response curves for LMD-009 (▼) and of the positive controls (■) selected among the possible endogenous chemokine agonists. The receptors were stimulated with the selected endogenous agonist at sub-maximal concentrations, aiming at 40 to 80% stimulation, for the antagonist test ($n = 3$).

that the right side of the LMD-009 molecule interacts with residues in the minor binding pocket (i.e., TyrI:07 and PheII:17, both located at the same level in the helices as VII:06) (Fig. 8A). The requirement for TyrI:07 has been described for several other nonpeptide antagonists targeting CCR1 and CCR5 (Tsamis et al., 2003; Seibert et al., 2006; Vaidehi et al., 2006). Thus, molecular modeling of CCR5 has suggested that TyrI:07 (Tyr^{37}) and TrpII:20 (Trp^{86}) constitute a large area of the small molecule interface as being in close proximity to the carboxyl group of GluVII:06 (Seibert et al., 2006).

The left side of LMD-009 is suggested to be in close proximity to and dependent upon TyrIII:08 in the major binding pocket as described for almost all characterized CC-chemokine receptor antagonists (Berkhout et al., 2003; Castonguay et al., 2003; de Mendonça et al., 2005; Maeda et al., 2006; Vaidehi et al., 2006) and position III:08—in the form of an Asp—is also a key-interaction point for the monoamines (Schwartz et al., 2006). The orientation of LMD-009 was mainly provided by studying the four analogs, LMD-584, LMD-902, LMD-268, and LMD-174, with variation in the left side compared with LMD-009, because they all reacted very differently from LMD-009 to mutations in the major binding pocket. Most notable are the effects of the mutations in PheVI:16 and TyrIII:09. Thus, in contrast to the 23-fold increase in the potency of LMD-009 for the substitution of PheVI:17 to Ala, we observed a 5- to 10-fold decrease for LMD-584 and LMD-902, whereas LMD-268 and LMD-174 were unaffected, and in contrast to LMD-009, all analogs depended on TyrIII:09; the two "elongated" amide-containing compounds were most affected (>25-fold decrease in potency for LMD-268 and LMD-174). The identified impact of PheVI:16 supports the notion that movement of TM-VI is important for receptor activation (Farrens et al., 1996; Schwartz et al., 2006). We suggest that the F254A mutation allows LMD-009 to reach deeper down into the pocket formed between TM-VI and TM-VII, thereby making an inward movement of TM-VI less restricted and favoring the active conformation of CCR8 (Schwartz et al., 2006). In contrast, LMD-584 and LMD-902 are directly dependent on PheVI:16, whereas the two "elongated" amide-containing LMD-268 and LMD-174 seem to be located more toward the pocket formed by TM-III and TM-IV, with no interference or interaction with Phe VI:16.

TrpVI:13 is highly conserved among rhodopsin-like 7TM receptors (71% contain Trp, 90% contain Trp, Phe, or Tyr) and is central for the activation mechanism in certain receptors (Shi et al., 2002; Schwartz et al., 2006). In CCR8, we observed no change in the agonist potencies upon mutating this residue, which, together with the fact that 6 of 21 chemokine receptors contain a Gln instead of the Trp, suggests that TrpVI:13 may not have the same impact on receptor activation as that observed in receptor families with smaller ligands (e.g., monoamines and ghrelin). This could be due to the large size (70–80 amino acids) and proposed superficial receptor interaction of the chemokines.

Chemokine Receptor Interaction with Peptide (Chemokine) versus Nonpeptide Agonist. Much effort has been made to describe the molecular mechanism of action of endogenous chemokines with their cognate receptors (Jarnagin et al., 1999; Schwarz and Wells, 2002). The three-dimensional structure of chemokines is well described, and the N terminus (before the two first conserved cysteines) is essen-

tial for receptor interaction (Hemmerich et al., 1999; Schwarz and Wells, 2002). However, the molecular interaction with the receptor is not yet known in detail. One prevailing model suggests that the chemokine N terminus docks into the receptor, whereas the core of the chemokine interacts with residues in the extracellular loops (Schwarz and Wells, 2002). Among the 29 mutations, we identified only two with selective importance for CCL1: W194A and G206A, located in the top and middle of TM-V, respectively. These positions, which are located in top of TM-V at the interface to the major binding pocket, fit with the putative docking of the N terminus of CCL1 into the major binding pocket.

Agonist-Prone 7TM Receptors. For the majority of 7TM receptors, high-throughput screening results in the identification of nonpeptide antagonists. Yet for a small fraction, nonpeptide agonists rather than antagonists appear. Some of these agonist-prone receptors display high constitutive activity (e.g., the ghrelin and melanocortin receptors), whereas others are more silent (e.g., somatostatin receptors) (Schwartz et al., 2006). The agonist-prone nature and the constitutive activity in these receptors are presumably determined by specific structural features in the receptors although these have not been identified yet. However, it is very likely that the mobility of TM-VI plays an important role as described in the global toggle switch model (Schwartz et al., 2006). CCR8 is an agonist-prone receptor, as judged by the discovery of nonpeptide agonists (LMD compounds and ZK 756326) and by the agonistic nature of the other vice antagonistic HHV8-encoded vCCL2 (Dairaghi et al., 1999). The agonist-prone nature of CCR8 was also supported by the observation that some of the mutations in the major binding pocket (especially Y172A and W251A/Q) and in the minor binding pocket (F84A and F290A) increased the basal signaling, independently of the surface expression (Table 1, Fig. 9). The impact of these mutations in the major binding pocket (and of F290A) is in good agreement with the global toggle switch model (Farrens et al., 1996; Schwartz et al., 2006), and the involvement of TM-II (F84A) in receptor activation has also been described previously for CC-chemokine receptors (Govaerts et al., 2001).

What Makes an Agonist an Agonist. In 7TM receptors the binding sites for small molecule ligands—agonists as well as antagonists—have repeatedly been located in the main ligand-binding pocket between the extracellular ends of the transmembrane helices (Schwartz et al., 2006). Yet, despite the fact that various differences have been described between agonists and antagonists in specific cases, the general molecular mechanism, which for some compounds leads to agonism and for others—even rather structurally similar compounds—leads to antagonism, has remained unclear. However, in the CXCR3 receptor, we have recently shown that small and simple compounds—bipyridine or phenanthrolene—could be turned into a highly efficacious agonist by ensuring that it, through an anchoring, silent metal-ion site, is tethered at a position corresponding to the binding site for β2-adrenergic agonists (i.e., between TM-III, TM-IV, and TM-V) (Rosenkilde et al., 2007). All together, these efficient nonpeptide agonists (in, for instance, CXCR3 and CCR8) are important tools for the elucidation of the mechanism of receptor activation, a prerequisite for rational design of efficient nonpeptide antagonists for 7TM receptors.

In the present study, we found that the small-molecule agonist LMD-009, like small-molecule antagonists in chemokine receptors in general, uses GluVII:06 as a major anchor point to interact with mainly aromatic key residues on each side (i.e., in the minor and major ligand-binding pockets, respectively). LMD-009 seems to bind relatively superficially in the pocket (Fig. 8A). Such a binding mode is in agreement with recent observations in the ghrelin receptor, where small peptide-based agonists also interact superficially in the corresponding area of the receptor, whereas compounds in which minor modification in the ligands allows for a deeper anchorage in the binding pocket are antagonists (Holst et al., 2006). It will therefore be extremely interesting to map the receptor binding sites of the recently published CCR8 small-molecule antagonists (Ghosh et al., 2006) in the near future.

Acknowledgments

We thank Lisbet Elbak, Randi Thøgersen, and Inger Smith Simonsen for excellent and skilful technical assistance. We thank Laura Storjohann for critical reading and fruitful discussion of the manuscript and Trond Ulven for chemical support.

References

Baldwin JM (1993) The probable arrangement of the helices in G protein-coupled receptors. *EMBO J* **12**:1693–1703.

Ballesteros JA and Weinstein H (1995) Integrated methods for the construction of three-dimensional models and computational probing of structure-function relations in G protein-coupled receptors, in *Receptor Molecular Biology* (Sealfon SC ed), pp 366–428, Academic Press, New York.

Berkhout TA, Blaney FE, Bridges AM, Cooper DG, Forbes IT, Gribble AD, Groot PH, Hardy A, Ife RJ, Kaur R, et al. (2003) CCR2: characterization of the antagonist binding site from a combined receptor modeling/mutagenesis approach. *J Med Chem* **46:**4070–4086.

Castonguay LA, Weng Y, Adolfsen W, Di Salvo J, Kilburn R, Caldwell CG, Daugherty BL, Finke PE, Hale JJ, Lynch CL, et al. (2003) Binding of 2-aryl-4-(piperidin-1-yl)butanamines and 1,3,4-trisubstituted pyrrolidines to human CCR5: a molecular modeling-guided mutagenesis study of the binding pocket. *Biochemistry* **42:**1544–1550.

Chensue SW, Lukacs NW, Yang TY, Shang X, Frait KA, Kunkel SL, Kung T, Wiekowski MT, Hedrick JA, Cook DN, et al. (2001) Aberrant in vivo T helper type 2 cell response and impaired eosinophil recruitment in CC chemokine receptor 8 knockout mice. *J Exp Med* **193:**573–584.

Dairaghi DJ, Fan RA, McMaster BE, Hanley MR, and Schall TJ (1999) HHV8-encoded VMIP-I selectively engages chemokine receptor CCR8. Agonist and antagonist profiles of viral chemokines. *J Biol Chem* **274:**21569–21574.

Damon I, Murphy PM, and Moss B (1998) Broad spectrum chemokine antagonistic activity of a human poxvirus chemokine homolog. *Proc Natl Acad Sci* **95:**6403–6407.

de Mendonça FL, da Fonseca PC, Phillips RM, Saldanha JW, Williams TJ, and Pease JE (2005) Site-directed mutagenesis of CC chemokine receptor 1 reveals the mechanism of action of UCB 35625, a small molecule chemokine receptor antagonist. *J Biol Chem* **280:**4808–4816.

Farrens DL, Altenbach C, Yang K, Hubbell WL, and Khorana HG (1996) Requirement of rigid-body motion of transmembrane helices for light activation of rhodopsin. *Science* **274:**768–770.

Gerard C and Rollins BJ (2001) Chemokines and disease. *Nat Immunol* **2:**108–115.

Ghosh S, Elder A, Guo J, Mani U, Patane M, Carson K, Ye Q, Bennett R, Chi S, Jenkins T, et al. (2006) Design, synthesis, and progress toward optimization of potent small molecule antagonists of CC chemokine receptor 8 (CCR8). *J Med Chem* **49:**2669–2672.

Govaerts C, Blanpain C, Deupi X, Ballet S, Ballesteros JA, Wodak SJ, Vassart G, Pardo L, and Parmentier M (2001) The TXP motif in the second transmembrane helix of CCR5. A structural determinant of chemokine-induced activation. *J Biol Chem* **276:**13217–13225.

Haskell CA, Horuk R, Liang M, Rosser M, Dunning L, Islam I, Kremer L, Gutierrez J, Marquez G, Martinez A, et al. (2006) Identification and characterization of a potent, selective nonpeptide agonist of the CC chemokine receptor CCR8. *Mol Pharmacol* **69:**309–316.

Hemmerich S, Paavola C, Bloom A, Bhakta S, Freedman R, Grunberger D, Krstenansky J, Lee S, McCarley D, Mulkins M, et al. (1999) Identification of residues in the monocyte chemotactic protein-1 that contact the MCP-1 receptor, CCR2. *Biochemistry* **38:**13013–13025.

Holst B, Lang M, Brandt E, Bach A, Howard A, Frimurer TM, Beck-Sickinger A, and Schwartz TW (2006) Ghrelin receptor inverse agonists: identification of an active peptide core and its interaction epitopes on the receptor. *Mol Pharmacol* **70:**936–946.

Horuk R (2003) Development and evaluation of pharmacological agents targeting chemokine receptors. *Methods* **29:**369–375.

Horuk R, Clayberger C, Krensky AM, Wang Z, Grone HJ, Weber C, Weber KS, Nelson PJ, May K, Rosser M, et al. (2001) A non-peptide functional antagonist of the CCR1 chemokine receptor is effective in rat heart transplant rejection. *J Biol Chem* **276:**4199–4204.

Jarnagin K, Grunberger D, Mulkins M, Wong B, Hemmerich S, Paavola C, Bloom A, Bhakta S, Diehl F, Freedman R, et al. (1999) Identification of surface residues of the monocyte chemotactic protein 1 that affect signaling through the receptor CCR2. *Biochemistry* **38:**16167–16177.

Javitch JA, Shi L, and Liapakis G (2002) Use of the substituted cysteine accessibility method to study the structure and function of G protein-coupled receptors. *Methods Enzymol* **343:**137–156.

Kostenis E (2001) Is Galpha16 the optimal tool for fishing ligands of orphan G-protein-coupled receptors? *Trends Pharmacol Sci* **22:**560–564.

Lüttichau HR, Stine J, Boesen TP, Johnsen AH, Chantry D, Gerstoft J, and Schwartz TW (2000) A highly selective CC chemokine receptor (CCR) 8 antagonist encoded by the poxvirus *Molluscum contagiosum. J Exp Med* **191:**171–180.

Maeda K, Das D, Ogata-Aoki H, Nakata H, Miyakawa T, Tojo Y, Norman R, Takaoka Y, Ding J, Arnold E, et al. (2006) Structural and molecular interactions of CCR5 inhibitors with CCR5. *J Biol Chem* **281:**12688–12698.

Mirzadegan T, Diehl F, Ebi B, Bhakta S, Polsky I, McCarley D, Mulkins M, Weatherhead GS, Lapierre JM, Dankwardt J, et al. (2000) Identification of the binding site for a novel class of CCR2b chemokine receptor antagonists: binding to a common chemokine receptor motif within the helical bundle. *J Biol Chem* **275:** 25562–25571.

Murphy PM, Baggiolini M, Charo IF, Hebert CA, Horuk R, Matsushima K, Miller LH, Oppenheim JJ, and Power CA (2000) International Union of Pharmacology. XXII. Nomenclature for chemokine receptors. *Pharmacol Rev* **52:**145–176.

Palczewski K, Kumasaka T, Hori T, Behnke CA, Motoshima H, Fox BA, Le T, I, Teller DC, Okada T, et al. (2000) Crystal structure of rhodopsin: a G protein-coupled receptor. *Science* **289:**739–745.

Rosenkilde MM, Andersen MB, Nygaard R, Frimurer TM, and Schwartz TW (2007) Activation of the CXCR3 chemokine receptor through anchoring of a small molecule chelator ligand between TM-III, -IV, and -VI. *Mol Pharmacol* **71:**930–941.

Rosenkilde MM, David R, Oerlecke I, ned-Jensen T, Geumann U, Beck-Sickinger AG, and Schwartz TW (2006) Conformational constraining of inactive and active states of a seven transmembrane receptor by metal ion site engineering in the extracellular end of transmembrane segment V. *Mol Pharmacol* **70:**1892–1901.

Rosenkilde MM, Kledal TN, Brauner-Osborne H, and Schwartz TW (1999) Agonists and inverse agonists for the herpesvirus 8-encoded constitutively active seven-transmembrane oncogene product, ORF-74. *J Biol Chem* **274:**956–961.

Rosenkilde MM and Schwartz TW (2006) GluVII:06—a highly conserved and selective anchor point for non-peptide ligands in chemokine receptors. *Curr Top Med Chem* **6:**1319–1333.

Schwartz TW (1994) Locating ligand-binding sites in 7TM receptors by protein engineering. *Curr Opin Biotech* **5:**434–444.

Schwartz TW, Frimurer TM, Holst B, Rosenkilde MM, and Elling CE (2006) Molecular mechanism of 7TM receptor activation—a global toggle switch model. *Annu Rev Pharmacol Toxicol* **46:**481–519.

Schwarz MK and Wells TN (2002) New therapeutics that modulate chemokine networks. *Nat Rev Drug Discov* **1:**347–358.

Schwede T, Kopp J, Guex N, and Peitsch MC (2003) SWISS-MODEL: an automated protein homology-modeling server. *Nucleic Acids Res* **31:**3381–3385.

Seibert C, Ying W, Gavrilov S, Tsamis F, Kuhmann SE, Palani A, Tagat JR, Clader JW, McCombie SW, Baroudy BM, et al. (2006) Interaction of small molecule inhibitors of HIV-1 entry with CCR5. *Virology* **349:**41–54.

Shi L, Liapakis G, Xu R, Guarnieri F, Ballesteros JA, and Javitch JA (2002) Beta2 adrenergic receptor activation. Modulation of the proline kink in transmembrane 6 by a rotamer toggle switch. *J Biol Chem* **277:**40989–40996.

Soler D, Chapman TR, Poisson LR, Wang L, Cote-Sierra J, Ryan M, McDonald A, Badola S, Fedyk E, Coyle AJ, et al. (2006) CCR8 expression identifies CD4 memory T cells enriched for FOXP3+ regulatory and Th2 effector lymphocytes. *J Immunol* **177:**6940–6951.

Trebst C, Staugaitis SM, Kivisakk P, Mahad D, Cathcart MK, Tucky B, Wei T, Rani MR, Horuk R, Aldape KD, et al. (2003) CC chemokine receptor 8 in the central nervous system is associated with phagocytic macrophages. *Am J Pathol* **162:**427–438.

Tsamis F, Gavrilov S, Kajumo F, Seibert C, Kuhmann S, Ketas T, Trkola A, Palani A, Clader JW, Tagat JR, et al. (2003) Analysis of the mechanism by which the small-molecule CCR5 antagonists SCH-351125 and SCH-350581 inhibit human immunodeficiency virus type 1 entry. *J Virol* **77:**5201–5208.

Vaidehi N, Schlyer S, Trabanino RJ, Floriano WB, Abrol R, Sharma S, Kochanny M, Koovakat S, Dunning L, Liang M, et al. (2006) Predictions of CCR1 chemokine receptor structure and BX 471 antagonist binding followed by experimental validation. *J Biol Chem* **281:**27613–27620.

Watson C, Jenkinson S, Kazmierski W, and Kenakin T (2005) The CCR5 receptor-based mechanism of action of 873140, a potent allosteric noncompetitive HIV entry inhibitor. *Mol Pharmacol* **67:**1268–1282.

Address correspondence to: Mette M. Rosenkilde, Laboratory for Molecular Pharmacology, Department of Pharmacology, The Panum Institute, Copenhagen University, Blegdamsvej 2, 2200 Copenhagen, Denmark. E-mail: rosenkilde@molpharm.dk